SUPPLEMENTAL FIGURE 1:

To discount the possibility that the reason that DNA-MIs; 5-azacytidine (vidaza) and 5-aza-2'deoxyctadine (decitabine) did not have a significant effect on cell growth was because they were unable to achieve significant physiological intra-cellular concentrations we assessed global changes in DNA-methylation using the EpigenTek Global Methylation Kit which allows the quantification of global DNA methylation through an ELISA-like reaction [1, 2] following 24 hours DNA-MI treatment. As seen in Supplemental Figure 1 (in which the global methylation state following treatment with either DNA-MI at either 1uM or 10uM is graphed as a percentage of the untreated baseline state), treatment with DNA-MI at either 1uM or 10uM is sufficient to significantly decrease global DNA methylation. These observations allow us to conclude that the DNA-MI dose 1uM is sufficient to result in physiological activity, but does not appear to affect cellular proliferation.

Methods:

Cells were incubated for 24 hours in the presence of 1uM decitabine. The concentrations of the HDACIs were identical to those represented in Figure 1A. Total genomic DNA was isolated from each cell line following treatment using the Qiagen Genomic DNA Isolation Kit. The Methylamp Universal Methylated DNA Preparation Kit [Base Cat. #P-1019] was used to generate a methylated positive control for each cell line. The EpigenTek Global Methylation Kit was used to quantitate global methylation levels in cell lines as a function of treatment. Briefly, as per the manufacturer's instructions: GM1 was diluted 1:10. Sample DNA concentration was adjusted to 6.6 ng/ul with GM2 and 30ul of DNA solution was added to each well in a 96 well plate. The plate frame was shaken to allow the solution to cover the whole surface of strip well bottom. The strip wells were incubated at 37°C (with no humidity) for 2 h followed by incubating at 60°C (no humidity) for 20-30 min to evaporate the solution and dry the wells. For the positive control, 29 µl of GM2 were added to the strip well followed by 1 µl of GM3 (100 ng/µl). Positive controls were generated by either using methylated DNA as obtained from the Methylamp Universal Methylated DNA Preparation Kit or by adding 29 µl of GM2 into the strip well followed by adding 1 µl of GM3 solution (100 ng/µl). Then to each well 150 µl of GM4 was added and incubated at 37°C for 30-45 min. The wells were aspirated and washed with 150 µl of the diluted GM1 three times. 50uM of GM5 (diluted at the 1:1000 ratio to 1 µg/ml) with the diluted GM1 was then added to each well and incubated at room temperature for 60 min. Finally all wells were

aspirated and washed with 150 µl of the diluted GM1 four times. GM6 was diluted (at 1:1000 ratio) with the diluted GM1. 50 µl of diluted GM6 was added to each well and incubate at room temperature for 30 min. Each well was aspirated and washed with 150 µl of the diluted GM1 five times. 100 µl of GM7 was added to each well and incubated at room temperature for 7 min in the dark. 50 µl of GM8 was added to each well. Absorbance was read on a microplate reader at 450 nm. The OD value was plotted versus the amount of GM3 to determine the slope. Then the amount of methylated DNA in each sample was calculated as: OD(sample-blank)/slope. The data was plotted as percentage of methylated DNA of the untreated sample. Each point was obtained three independent times and the average and standard deviation is plotted.

Supplemental Figure 1 Legend:

Global DNA-methylation assay was determined using EpigenTek DNA methylation kit was used per manufacturer's instructions. The Y-axis represents the amount of methylated DNA as a percentage of the untreated sample. X-axis represents the panel of sarcoma cell lines following treatment with either with 1uM or 10uM of the two DNA-MIs vidaza (V) or decitabine (D) for 24 hours.

SUPPLEMENTAL FIGURE 2:

To examine whether HDACI activity correlated with its inhibitory effect on cellular growth, we assessed global changes in histone acetylation using the EpigenTek Global Histone H3 Acetylation Kit [3, 4]. Cells were treated with each of the five HDACIs within a similar spectrum used for the cell proliferation assays (Figure 1A) and treated for 24 hours. In general, after greater than 24 hours of treatment and at the higher doses (please see Supplemental Figures 3-5) of the dosage spectrum of each HDACI significant cellular debris was noted. In order to ensure that cellular death did not confound HDACI activity measurements, we assayed HDACI activity following 24 hours of treatment. As seen in Supplemental Figure 2, each HDACI is able to achieve an increase in histone acetylation at doses approximately 10 fold lower at which cellular growth inhibition is observed. Please compare Supplemental Figure 2 to Figure 1.

Methods:

The EpiQuik Global Histone H3 Acetylation Assay Kit [Base Cat. #P-4008] was used to assess changes in global histone acetylation. Briefly, the acetylated histone H3 is recognized with a

high-affinity antibody and the ratio of acetylated histone H3 is quantified through HRP conjugated secondary antibody-color development system. The protocol is similar to the one outlined in detail for DNA-methylation in the Methods of Supplemental Figure 1. Each sample and its controls were repeated three times. The values were averaged and graphed. Standard deviation bars are shown. The percentage difference was determined by dividing the averaged IC50 for each HDACI in the absence vs. the averaged IC50 in the presence of decitabine. Significance was assessed with Student's t-test. Differences in measurements were considered significant at $p < 0.05$.

Supplemental Figure 2 Legend:

HDACI activity represented as fold change of the untreated cell line (control) is plotted on the Y-axis. Sarcoma cell lines following treatment with the indicated HDACI are plotted on the X-axis. All points indicate activity 24 hours of HDACI treatment. Each sample and its controls were repeated three times. The values were averaged and graphed. Standard deviation bars are shown.

SUPPLEMENTAL FIGURE 3:

As an initial step in determining the cause underlying the inhibition of cell growth observed in the presence of epigenetic agents (MTS assays Figure 1A and crystal violet assays) we performed trypan blue staining as a viability assay on our sarcoma cell panel as a function of the dose of the HDACI in the absence or presence of the DNA-MI decitabine. The trypan blue exclusion test of cell viability is used to determine the number of viable cells present in a cell suspension. It is based on the principle that live cells possess intact cell membranes that exclude certain dyes, such as trypan blue, whereas dead cells do not. In this test, a cell suspension is mixed with dye and then visually examined to determine whether cells take up or exclude dye. A viable cell will have a clear cytoplasm whereas a nonviable cell will have a blue cytoplasm.

Cells were treated for 72 hours in a similar manner as outlined for the MTS assays described in Figure 1A and viability determined immediately afterwards as outlined in the methods section below. In Supplemental Figure 3 we graphically represent the number of live cells as a percentage of the total observed cells. As seen in Supplementary Figure 3, cells maintain their viability at the previously noted respective IC50s. Furthermore, in the ESR cell

lines, there is a noted increase in the loss of viability, but again the loss of viability occurs at doses higher than the respective IC50s. Please compare Supplemental Figure 3 to Figure 1A. These results indicate that at the IC50, epigenetic agents mediate primarily a cytostatic, rather than cytotoxic effect, however at doses above the IC50 cytotoxicity is observed. Finally, all reactions were repeated at 24 hours as well as 48 hours of epigenetic agent treated (data not shown); however significant loss of viability was only observed at 72 hours.

Methods:

Cells were plated as described in the Materials and Methods of the main text. 0.4% trypan blue was purchases from Gibco/BRL. Cells were incubated for three days with either HDACIs alone or with HDACIs in the presence of 1uM decitabine. The concentrations of the HDACIs were identical to those represented in Figure 1A. Cells were counted and a 1ml aliquot in PBS containing approximately $5x10^5$ cells was prepared. Cells were then mixed 1 part 0.4% trypan blue and 1 part cell suspension and allowed to incubate 3 minutes at room temperature. Immediately upon completion of this incubation period a drop of the trypan blue/cell mixture was observed in a hemacytometer. The hemacytometer was placed on the stage of a binocular microscope and the unstained (viable) and stained (nonviable) cells were counted separately. To obtain the total number of viable cells per ml of aliquot, the total number of viable cells was multiplied by 2 (the dilution factor for trypan blue). To obtain the total number of cells per ml of aliquot, the total number of viable and nonviable cells were added and multiplied by 2. In Figure 3 we graphically represent the number of live cells as a percentage of the total counted cells. Each experiment was performed three independent times and the average and standard deviation are shown.

Supplemental Figure 3 Legend:

The Y-axis represents percentage viability as determined as the number of live cells divided by the total counted cells. The X-axis represents sarcoma cell lines treated with each HDACI in the absence or presence of decitabine. The bar graphs represent treatment with the indicated drugs and doses as represented on the graphs. Each sample and its controls were repeated three times. The values were averaged and graphed. Standard deviation bars are shown.

SUPPLEMENTAL FIGURE 4:

To independently confirm that epigenetic agents mediate primarily a cytostatic rather than cytotoxic effect at the IC50, we performed a cell cycle analysis on our sarcoma cell line panel as a function of the dose of the HDACI in the absence or presence of the DNA-MI decitabine following 72 hours of epigenetic agent treated. As seen in Supplementary Figure 4, as the HDACI dose approximates the IC50 sarcoma cell lines primarily accumulate in G1. During this time there is a corresponding decrease in the percentage of cells in S and G2 (data not shown in order to draw focus to G1 and sub-G1 fractions); and there is no evidence of cells accumulating in sub-G1 (the latter an indication of apoptotic or necrotic cells). However, as the HDACI dose increases over the IC50, the percentage of cells in G1 begin to decrease and the percentage of cells accumulating in sub-G1 increase greatly. Again, in the ESR cell lines , both the accumulation in G1 at the IC50 as well as the sub-G1 peaks observed at higher concentrations are accentuated by the addition of the DNA-MI. These results are in accordance with the viability data observed in Supplemental Figure 3 and together suggest that at the IC50, epigenetic agents predominantly result in a cytostatic effect via an accumulation in G1. Finally, all reactions were repeated at 24 hours as well as 48 hours of epigenetic agent treated (data not shown). Significant changes in cell cycle were best detected at the 72 hour time point shown in Supplemental Figure 4.

Methods:

Cells were plated as described as described in the Materials and Methods of the main text and treated for 72 hours with the indicated HDACIs (at the range of concentrations shown in Figure 1A) in the absence and presence of the DNA-MI decitabine. Following 72 hours of treatment all cells (attached and unattached) were collected and fixed with 2% fresh formaldehyde in PBS for 5-15 minutes while gently rotating. The cells were subsequently washed three times with PBS and resuspended in 300ul of PBS to which 700ul of 100% -20 EtOH was added. The cells were subsequently spun at 5000RPM for five minutes and washed with PBS. Finally cells were resuspended in 1ml of 2.5ug/ml propidium iodide and 0.5 mg/ml RNase A in PBS. The samples were placed in 5ml FACS tubes and cell cycle analysis was performed on the BD FACSCalibur multicolor flow cytometer within the Columbia Cancer Center FACS facility. Each sample and its controls were repeated three times. The values were averaged and graphed. Standard deviation bars are shown.

Supplemental Figure 4 Legend:

The Y-axis represents the percentage of cells in the indicated phase of the cell cycle (either sub-G1 or G1). The X-axis represents sarcoma cell lines treated with each HDACI in the absence or presence of decitabine. The bar graphs represent treatment with the indicated drugs and doses as represented on the graphs. Each sample and its controls were repeated three times. The values were averaged and graphed. Standard deviation bars are shown.

SUPPLEMENTAL FIGURE 5:

To examine whether the sub-G1 peak observed at HDACI concentrations above the IC50 were the result of the accumulation of necrotic or apoptotic cells, we assayed for the presence of Caspase 3. Caspase 3 was chosen as it is an active cell-death protease involved in the execution phase of apoptosis, during which cells undergo changes such as DNA fragmentation, chromatin condensation, and apoptotic body formation. Caspase 3 is activated in response to multiple stimuli including serum withdrawal, activation of Fas, treatment with radiation and pharmacological agents as well as to other upstream caspases such as caspase-8 and caspase-9.

Cells were treated for 72 hours in a similar manner as outlined for the MTS assays described in Figure 1A and Caspase 3 activity determined using the ApoAlert Caspase 3 Fluorescent Assay (please see methods below). In Supplemental Figure 5 we graphically represent the caspase 3 activity as fold change above the control, here defined as that activity in the untreated cells. As could be seen in Supplemental Figure 5, significant accumulation of Caspase-3 does not appear at doses at which cell growth inhibition is observed but at doses higher than the IC50. Please compare Supplemental Figure 5 to Figure 1A. The appearance of caspase-3 activity does however correspond to the appearance of the sub-G1 peak observed in Supplemental Figure 4. Staurosporine (as an apoptotic inducing agent) as well as the caspase-3 inhibitor (DEVD-CHO) were used as controls for these reactions (please see Methods below). Finally, all reactions were repeated at 24 hours as well as 48 hours of epigenetic agent treated (data not shown). Significant caspace-3 activity was best detected at the 72 hour time point shown in Supplemental Figure 5.

Methods:

The ApoAlert Caspase 3 Fluorescent Assay activity was used as follows per the manufacturer's instructions. $1x10^6$ cells were incubated for three days with either HDACIs alone or with HDACIs in the presence of 1uM decitabine. The concentrations of the HDACIs were identical to those represented in Figure 1A. Control plates included cells in the absence of epigenetic agents (negative control) and cells in the presence of staurosporine 500nM. Due to staurosporine's potent and rapid apoptotic action, cells were treated for 8 hours in order to establish apoptotic cells as a positive control for the caspase-3 assay. At the end of 72 hours of treatment, cells were centrifuged at 400g for 5 minutes and resuspended in 50ul of chilled cell lysis buffer and incubated on ice for 10 minutes. Cell lysates were centrifuged at maximum speed for 10 minutes at 4C and supernatant transferred to new tubes. 50ul of 2X Reaction Buffer/DTT mix and 1uL caspase-3 inhibitor (DEVD-CHO) was then added to 50ul of the supernatant to act as a further positive control to the assay. Similarly a mock 1uL DMSO was added to a separate 50ul of reaction along with 50ul of 2X Reaction Buffer. To each tube 5ul of 1mM of a 50uM Caspase-3 substrate (DEVD-AFC) was added. The reaction was incubated at 37C for 1hour. The samples were then all transferred to a 96 well plate and read in fluorometer with 400nm excitation filter and 505nm emission filter. Each sample and its controls were repeated three times. The values were averaged and graphed. Standard deviation bars are shown.

Supplemental Figure 5 Legend:

The Y-axis represents caspase 3 activity plotted as fold change above the control. The control is defined per cell line as the caspase 3 activity of the untreated cells. The X-axis represents sarcoma cell lines treated with each HDACI in the absence or presence of decitabine. The bar graphs represent treatment with the indicated drugs and doses as represented on the graphs. Each sample and its controls were repeated three times. The values were averaged and graphed. Standard deviation bars are shown.

SUPPLEMENTAL FIGURE 6:

Please see main text and methods for details regarding in vivo treatment. Treated mice were sacrificed either early (Day 5) in the treatment schedule to allow for characterization of any early changes that may potentially be obscured by prolonged treatment; as well as late (Day 21) in the treatment schedule. In both cases, mice were sacrificed within 24 hours of treatment.

To explore in detail the changes that were occurring to the xenografts as a result of epigenetic treatment, tumors were extracted from the sacrificed mice, paraffin embedded and analyzed. The time from last treatment to tumor extraction was less than 24 hours. Tumors were quartered and multiple slides prepared and analyzed from all quarters. No signs of necrosis were observed either grossly or in any of the quarters or in the hematoxylin and eosin prepared slides in any of the xenografts from either untreated or epigenetically treated mice (Supplemental Figure 6). The lack of observed necrosis at the histologic level, but the readily measurable difference in growth rates of the xenografts (Figure 2) suggests that in vivo epigenetic agents mediate primarily a cytostatic effect on sarcoma cells. These results are in agreement with our in vitro data at concentrations approximating the IC50.

Methods:

Treated mice were sacrificed either early (Day 5) in the treatment schedule to allow for characterization of any early changes that may potentially be obscured by prolonged treatment; as well as late (Day 21) in the treatment schedule. In both cases, mice were sacrificed within 24 hours of final treatment. Tumors were fixed in 10% formalin, embedded in paraffin and stained with hematoxylin and eosin as previously described [5]. Please see main text and methods for details regarding in vivo treatment

Supplemental Figure 6 Legend:

Hematoxylin and eosin stained representative slides of untreated and epigenetically treated SKUT1 and SKUT1B xenografts taken at day 5 (D5) and day 21 (D21) of treatment are shown. Tumors shown were prepared within 24 hours of last epigenetic treatment.

SUPPLEMENTAL FIGURE 7:

Please see main text and methods for details regarding in vivo treatment and xenograft preparation. Since no necrosis was observed grossly or upon hematoxylin and eosin staining, we performed immunohistochemistry for Ki67. Although Ki67 is a commonly used tumor proliferative index [6] it has not always proven to absolutely correlate with cellular proliferation [7]. We have however assessed the relationship between in vivo growth and ki67 in a large panel of sarcoma cell lines [5]. In that report we performed a linear regression analysis represented as pair-wise plots and found that given that a coefficient of correlation equaling "1" represents identity, the association between in vivo Ki67 and in vivo days to tumor formation is 0.64. This correlation is suggestive of a direct, albeit not perfect relationship.

Having established that Ki67 associates with proliferation, we prepared slides from xenografts as described in main Text and Methods, as well as Supplemental Figure 6 Text and immunohistochemically analyzed those slides for the presence of Ki67. As described in the main text, loss of Ki67 decreased in response to both valproate and SAHA and in both cell lines. However when SAHA or valproate was combined with decitabine, Ki67 staining cells were rarely found in SKUT1 xenografts by day five, and completely absent on day 21. In contrast, SKUT1B cells continued to have Ki67 staining positive cells even at day 21 of treatment, although those levels were significantly reduced as compared to untreated samples (Figure 2E, compare SKUT1 vs SKUT1B Day5 and Day 21 (yellow SAHA+Dec) and light blue (Valproate+Dec) bars,and Supplemental Figure 7 green and red boxes.)

Methods:

Tumors were fixed in 10% formalin, embedded in paraffin and stained for Ki67 (rabbit polyclonal; ab15580; Abcam) as previously described [5, 8].

Supplemental Figure 7 Legend:

Ki67 stained representative slides of untreated and epigenetically treated SKUT1 and SKUT1B xenografts taken at day 5 (D5) and day 21 (D21) of treatment are shown. Tumors shown were prepared within 24 hours of last epigenetic treatment. Green box= SKUT1B double agent treated xenografts; Red box= SKUT1 double agent treated xenografts. Please see text above for appropriate comparisons.

SUPPLEMENTAL FIGURE 8:

Please see main text and methods for details regarding in vivo treatment and xenograft preparation. To assess that HDACI treatment was physiologically affecting the tumor, we immunohistochemically assayed the epigenetically treated tumors as well as controls for changes in histone H3 acetylation. As can be observed in Supplemental Figure 8, treatment with valproate and SAHA was only able to increase the overall Histone H3 acetylation modestly (compare untreated (purple boxes) to valproate and SAHA treated xenografts (green boxes); Supplemental Figure 8). However, in the presence of decitabine, the ability of valproate and SAHA to significantly increase Histone H3 acetylation is readily noted (red boxes). Finally, we also noted that the increase in Histone H3 acetylation in response to combined HDACI/DNA-MI treatment was much more pronounced for SKUT1 (lower two panels far right, Supplemental Figure 8); as opposed to SKUT 1B (upper two panels far right, Supplemental Figure 8).

Methods:

Tumors were fixed in 10% formalin, embedded in paraffin and stained for acetylated Histone H3 (AcH3; Cell Signaling, Cat # 9677S) per standard protocol as previously described [5, 8].

Supplemental Figure 8 Legend:

Acetylated Histone H3 stained representative slides of untreated and epigenetically treated SKUT1 and SKUT1B xenografts taken at day 5 (D5) and day 21 (D21) of treatment are shown. Tumors shown were prepared within 24 hours of last epigenetic treatment. Purple box=untreated xenografts; Green box=HDACI treated xenografts; Red box=combined epigenetic treatment. Please see text above for appropriate comparisons.

Supplemental Figure 9:

Please see main text and methods for details regarding in vivo treatment and xenograft preparation. To assess changes in p21 (a cyclin dependent kinase inhibitor previously characterized to be a HDACI responsive gene [9], we performed an immunohistochemical analysis for p21 in untreated and epigenetically treated xenografts. We noted that the expression of p21 was upregulated by both HDACIs (but not by decitabine) and only in SKUT1 cells (Figure 2E and Supplemental Figure 9, blue box). Furthermore, only SKUT1 cells were

able to show a synergistic response as noted by further increase in p21 in the presence of combined HDACI/DNA-MI (Figure 2E and supplemental Figure 8; compare green and red boxes).

Methods:

Tumors were fixed in 10% formalin, embedded in paraffin and stained for p21/waf1 (Calbiochem, Cat # OP64), per standard protocol as previously described [5, 8].

Supplemental Figure 9 Legend:

p21 stained representative slides of untreated and epigenetically treated SKUT1 and SKUT1B xenografts taken at day 5 (D5) and day 21 (D21) of treatment are shown. Tumors shown were prepared within 24 hours of last epigenetic treatment. Please see text above for appropriate comparisons.

Supplemental Figure 10:

To confirm our hypothesis that an inverse ratio of CUGBP2 to RHOJ would not be found in those cell lines showing a mixed response to the various HDACIs when combined with decitabine in terms of synergy, we performed both a quantitative RT-PCR and immunoprecipitation-immunoblotting of either CUGBP2 or RHOJ in the cell lines showing a mixed response: SKNEP, SW872, OSA, RH30, and HOS. As could be seen in Supplemental Figure 10A,B, none of these five cell lines exhibit a similar inverse relationship as observed for both the ESR and non-ESR cell lines seen in Figure 3C,D.

To assess the changes to CUGBP2 and RHOJ following epigenetic therapy we treated our sarcoma cell line panel with both decitabine and the HDACIs as single agents, as well as combination therapies and performed ELISA assays for either CUGBP2 or RHOJ. All treatments were either for 24 or 72 hours. Since there was little difference observed between the 24 and 72 hour treatments, 24 hour time points are shown in Supplemental Figure 10C,D. As seen in Supplemental Figure 10C,D, CUGBP2 decreased (approximately 40%) and RHOJ increased (approximately 30-40%) in response to combined epigenetic therapy for the ESR cell lines only. These differences were statistically significant.

Methods:

Quantitative RT-PCR and immunoprecipitation-immunoblotting of either CUGBP2 or RHOJ were performed as described in the main Methods section.

Sandwich ELISA for CUGBP2 or RHOJ following either 24 or 72 hour treatments with epigenetic agents were performed as following using the following antibodies:

CUGBP2: Mouse Anti-CUG-BP1/2 Monoclonal antibody, Unconjugated, Clone b-1, (Santa Cruz Biotechnology, Inc. and Rabbit Anti-CUGBP2 Polyclonal, Unconjugated (Novus Biologicals). CUGBP2 Recombinant Protein (H00010659-P01 a.a. 1 - 521 a.a.) full-length recombinant protein with GST tag (Abnova) was used as a positive control.

RHOJ: Mouse Anti-Human RHOJ Monoclonal antibody, Unconjugated, 1E4 (Abnova Corporation) and Rabbit Anti-Human Rhoj Polyclonal antibody, Unconjugated (Atlas Antibodies). RHOJ Recombinant Protein (H00057381-P01, 1 a.a. - 215 a.a.) full-length recombinant protein with GST tag (Abnova) was used as a positive control.

Cells were cultured as previously described. Trypsinized, pelleted and incubated in the following cell lysis buffer: 20 mM Tris (pH 7.5), 150 mM NaCl, 1 mM ethylene diamine tetraacetate (EDTA), 1 mM ethylene glycol-bis(2-aminoethyl)-N,N,N′,N′-tetraacetic acid (EGTA), 1% Triton X-100, 2.5 mM sodium pyrophosphate, 1 mM β-glycerophosphate, 1 mM Na3VO4, 1µg/ml leupeptin.

A capture antibody, indicated above, is first diluted in 0.1M Bicarbonate buffer, pH 9.2 and then 50 µl is added to each well of the microtiter plate. The antibody coated plate is covered with Paraffin and incubated in the cold room overnight. The plate is emptied and the unoccupied sites are blocked with 100 µl of blocking buffer containing 100 mM phosphate buffer, pH 7.2, 1% BSA, 0.5% Tween-20 and 0.02% Thimerosol for 30 min at room temperature. The plate is emptied and washed three times with wash buffer(100 mM phosphate buffer, 150 mM NaCl, 0.2% BSA and 0.05% Tween 20). The antigen solution is first diluted in antigen buffer (100 mM phosphate buffer, 150mM NaCl) and then added to the plate in a volume of 50 µl per well. The plate is incubated at room temperature for one hour. The plate is emptied again and washed three times with wash buffer. A Polyclonal Antibody, Unconjugated as indicated above is diluted appropriately in 0.1M Bicarbonate buffer, pH 9.2 and then 50 µl is added to each well and incubated at room temperature for 30 min. The plate is emptied again and washed three times with wash buffer.

Significance was calculated using Student's t-test.

Supplemental Figure 10 Legend:

(A) Quantitative RT-PCR of either CUGBP2 or RHOJ. (B) immunoprecipitation-immunoblotting of either CUGBP2 or RHOJ on cell lines showing mixed synergy response to HDACI/DNA-MI treatment. (C,D) ELISA for RHOJ and CUGBP2 from total cellular extracts obtained from the indicated cell lines following the indicated treatments for 24 hours. The untreated level was set at baseline, arbitrarily assigned as 1. All subsequent values were normalized to the baseline of each cell, and plotted on the Y-axis as relative quantity. Each graph shows an average of six individual extracted samples. Standard error is shown as bar graphs. *=$p<0.05$.

Supplemental Figure 11:

To formally assess if CUGBP2 and RHOJ were markers or potential effectors of epigenetic responsiveness we downregulated either CUGBP2 in ESR cell lines SAOS2,SKUT1 and MFH; or downregulated RHOJ in non-ESR cell lines SW982, SKUT1B and LS141 using small interference RNA.

As could be seen in sandwich ELISA in Supplemental Figure 11A, treatment of cell lines SAOS2, SKUT1 and MFH with CUGBP2 siRNA significantly downregulated CUGBP2 levels, without significantly affecting the levels of CUGBP2 in SW982, SKUT1B and LS141 cell lines (presumably as demonstrated in Figure 3C,D because these cell lines have low levels of CUGBP2 to begin with (compare first set of six bars to second set of six bars in Supplemental Figure 11A). As a control for siRNA-CUGBP2 specificity, treatment with siRNA-RHOJ had no effect on CUGBP2 levels (compare first set of six bars with third set of six bars, Supplemental Figure 11A).

Similarly as could be seen in Supplemental Figure 11B, treatment of cell lines SW982, SKUT1B and LS141 with RHOJ-siRNA significantly downregulated RHOJ levels, without significantly affecting the levels of RHOJ in SAOS2, SKUT1 and MFH cell lines (presumably as demonstrated in Figure 3C,D because these cell lines have low levels of RHOJ to begin with (compare first set of six bars to second set of six bars in Supplemental Figure 11B. As a control for siRNA-RHOJ specificity, treatment with siRNA-CUGBP2 had no effect on RHOJ levels (compare first set of six bars with third set of six bars, Supplemental Figure 11B).

Having shown that the specificity of our targeted downregulation of either CUGBP2 in ESR cell lines or RHOJ in non-ESR cell lines (Supplemental Figure 11A, B), we went on to test

the effect of changes in these genes on epigenetic responsiveness. 24 hours of after CUGBP2-siRNA transfection of the ESR cell line SAOS2 or RHOJ-siRNA transfection of the non-ESR cell line SW982, we further treated each cell line with either the five HDACIs alone or in combination with decitabine for 72 hours as described for Figure 1A.

As could be seen Supplemental Figure 11C, downregulating CUGBP2 in SAOS2 does not abolish the epigenetic synergy observed (note that each original curve, one corresponding to HDACI treatment alone and the other corresponding to HDACI with decitabine, now run as doublets). We would have expected that if epigenetic synergism was abolished following downregulation of CUGBP2, then the HDACI+decitabine+siRNA-CUGBP2 line would overlap with the HDACI arm, however that effect was not observed,

As seen in Supplemental Figure 11D, downregulating RHOJ in SW982 did not instate epigenetic synergy (note that each original curve, one corresponding to HDACI treatment alone and the other corresponding to HDACI with decitabine - which previously ran as an almost overlapping doublet now run as four overlapping lines. We would have expected that if epigenetic synergism was established that the lines would separate and that the HDACI+decitabine+siRNA-RHOJ would run as an independent line, however that effect was not observed.

Methods:

Production of retroviral supernatants was carried out by calcium phosphate-mediated transfection of amphotropic packaging Phoenix cells. High-titer retroviral supernatants were passed through a 0.45 μm filter and supplemented with 1μg/ml polybrene (Sigma) and transferred to the indicated cell lines. siRNAs for CUGBP2 and RHOJ were purchased from Qiagen (Xeragon) and transfected using the HiPerFect Transfection Reagent (Qiagen). Sandwich ELISA assays for CUGBP2 and RHOJ were done as described in the Methods of Supplemental Figure 10. Mock and scrambled siRNA transfections were carried out as controls and used as baseline from which change was calculated.

The cell lines SAOS2 and SW982 were transfected as described above. 24 hours later, media was changed and the cells treated with either HDACI alone or with HDACI+decitabine at a range of concentrations as described for Figure 1A. MTS assays were measured at 72 hours after treatment. Control was mock transfected and grown in the absence of epigenetic agents.

Supplemental Figure 11 Legend:

ELISA for CUGBP2 (A) and RHOJ (B) CUGBP2 from total cellular extracts obtained from the indicated cell lines following the indicated siRNA transfections of either siRNA CUGBP2 or siRNA RHOJ. The control (mock and scrambled) level was set at baseline, arbitrarily assigned as 1 (left). All subsequent values were normalized to the baseline of each cell, and plotted on the Y-axis as relative quantity. Each graph shows an average of three individual samples. Standard error is shown as bar graphs. (C,D) MTS/cell viability assays of the indicated cell lines treated with the indicated epigenetic agents. The Y-axis represents "cell proliferation" plotted as a fraction of the proliferation of the untreated cell line. The X-axis represents the individual cell lines treated with the indicated epigenetic agents at the dose ranges and combinations indicated on the graphs. Each point was assayed three independent times. Average is shown and error bars represent standard deviation at each point.

REFERENCES (to supplement):

1. Blazkova, J., et al., *CpG methylation controls reactivation of HIV from latency.* PLoS Pathog, 2009. **5**(8): p. e1000554.
2. Chen, C., et al., *Aberrant DNA methylation in thymic epithelial tumors.* Cancer Invest, 2009. **27**(5): p. 582-91.
3. Kobori, A., et al., *Butyrate stimulates IL-32alpha expression in human intestinal epithelial cell lines.* World J Gastroenterol, 2010. **16**(19): p. 2355-61.
4. Hu, N., et al., *Abnormal histone modification patterns in lupus CD4+ T cells.* J Rheumatol, 2008. **35**(5): p. 804-10.
5. Mills, J., et al., *Characterization and comparison of the properties of sarcoma cell lines in vitro and in vivo.* Hum Cell, 2009. **22**(4): p. 85-93.
6. Heslin, M.J., et al., *Ki-67 detected by MIB-1 predicts distant metastasis and tumor mortality in primary, high grade extremity soft tissue sarcoma.* Cancer, 1998. **83**(3): p. 490-7.
7. Brown, D.C. and K.C. Gatter, *Ki67 protein: the immaculate deception?* Histopathology, 2002. **40**(1): p. 2-11.
8. Matushansky, I., et al., *Derivation of sarcomas from mesenchymal stem cells via inactivation of the Wnt pathway.* J Clin Invest, 2007. **117**(11): p. 3248-3257.
9. Richon, V.M., et al., *Histone deacetylase inhibitor selectively induces p21WAF1 expression and gene-associated histone acetylation.* Proc Natl Acad Sci U S A, 2000. **97**(18): p. 10014-9.

Supp FIGURE 1:

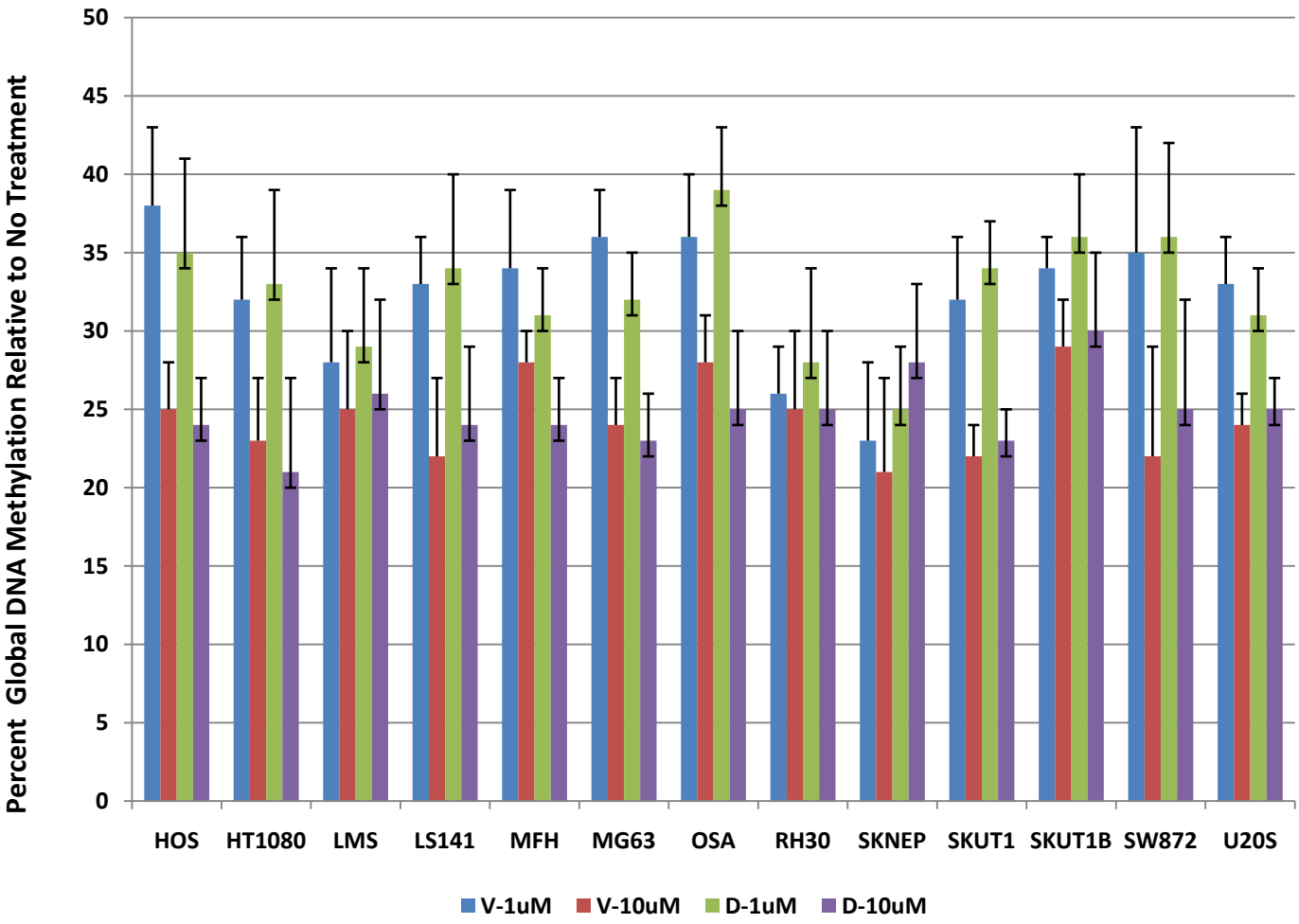

Supp FIGURE 2:

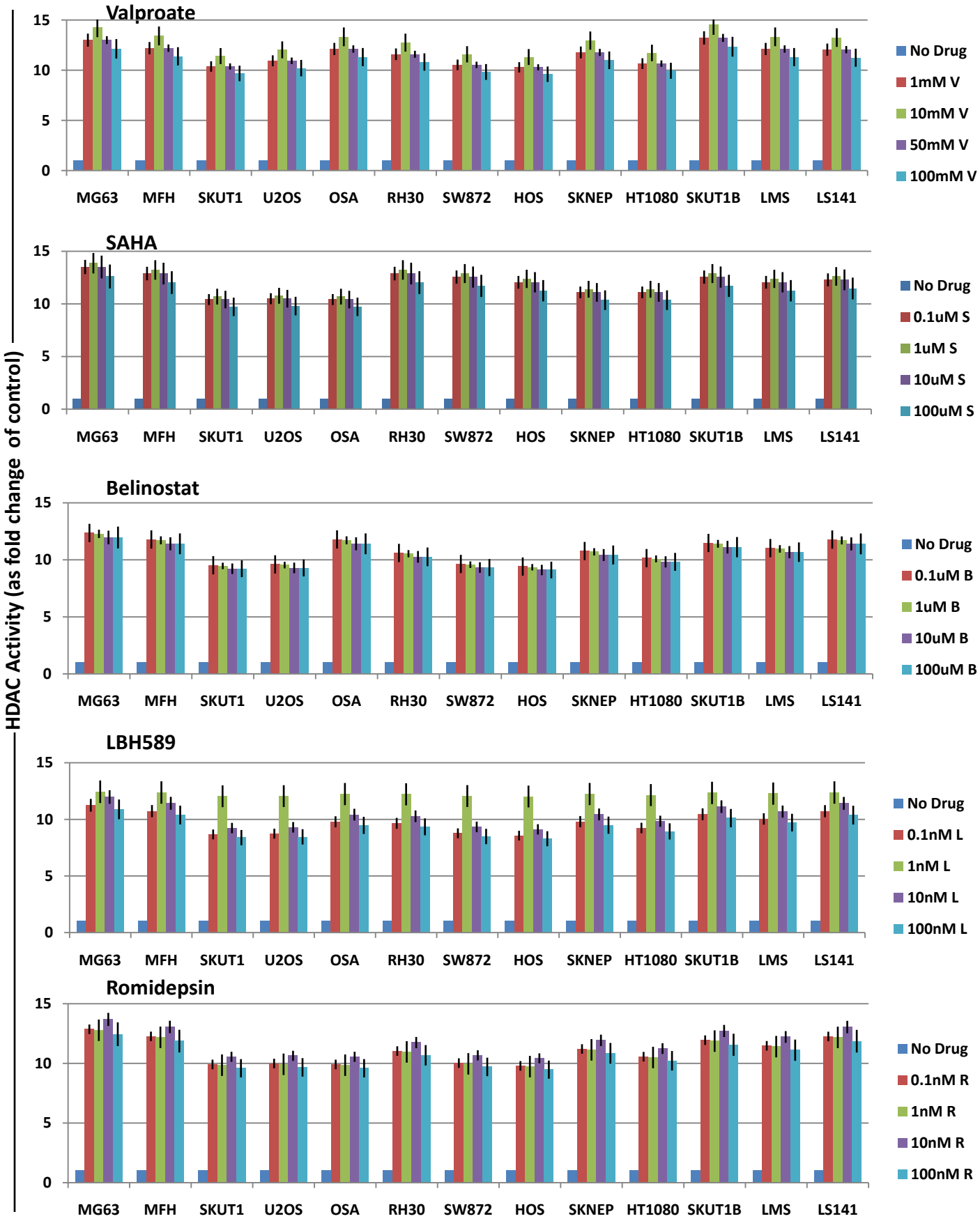

Supp FIGURE 3:

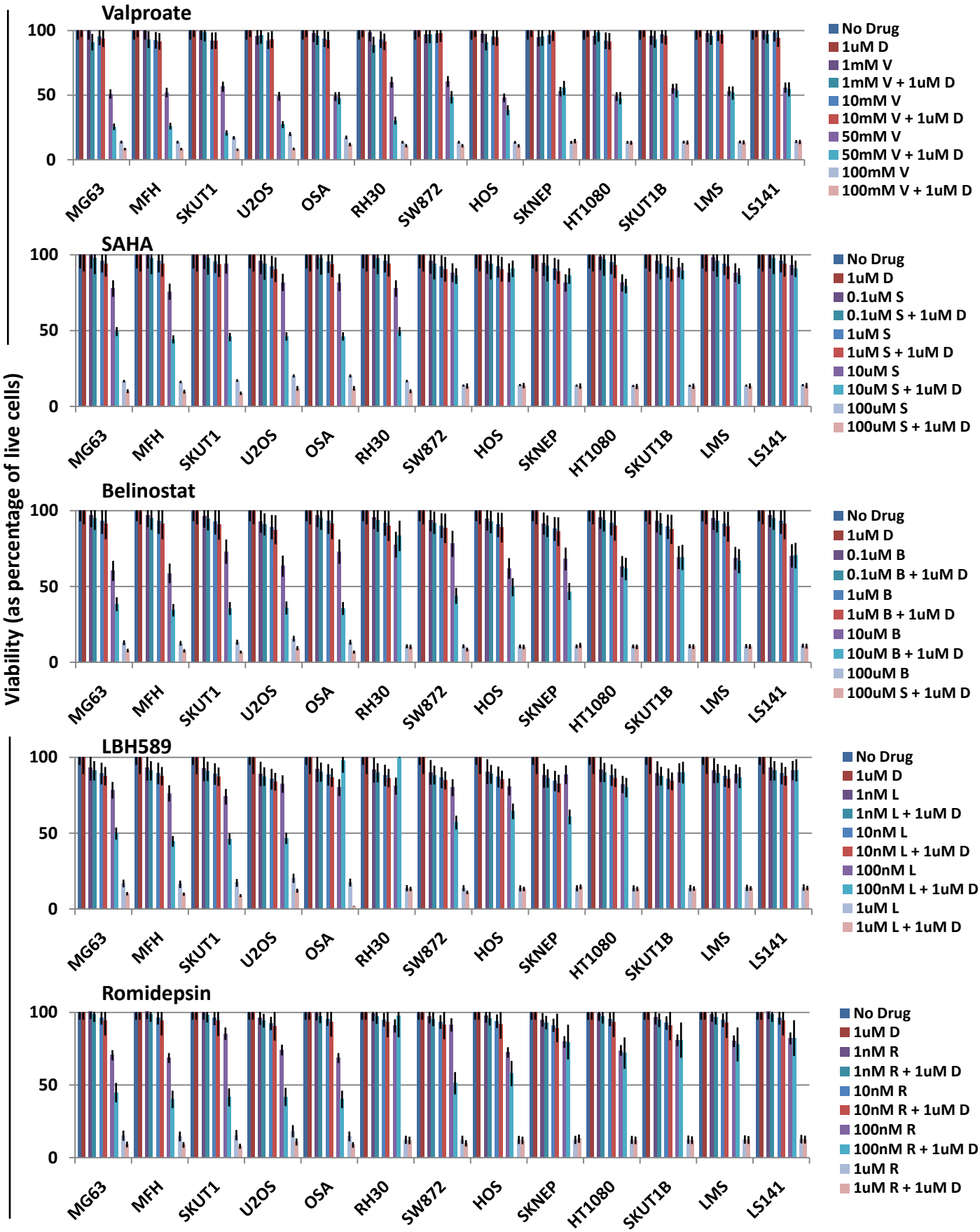

Supp FIGURE 4:

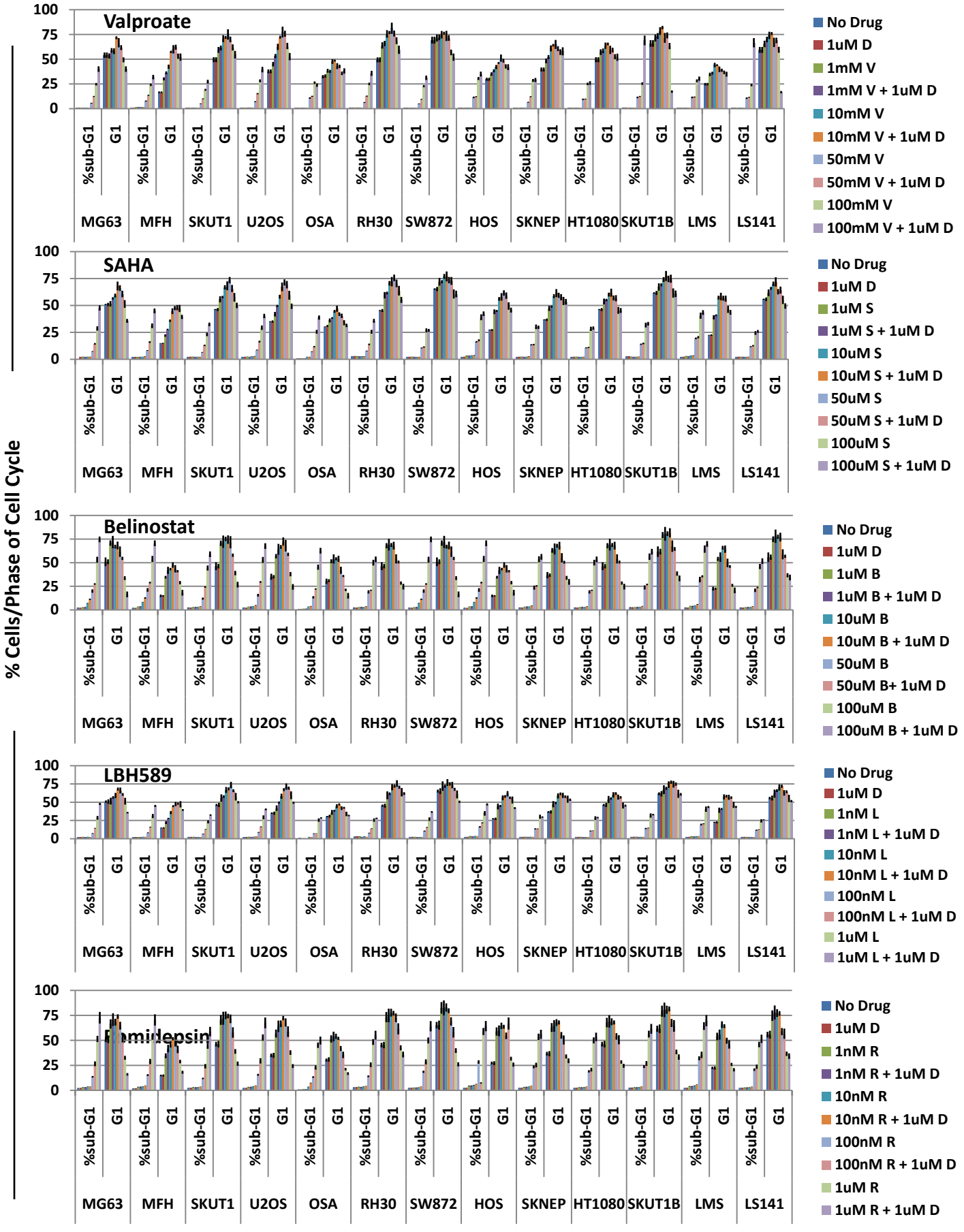

Supp FIGURE 5:

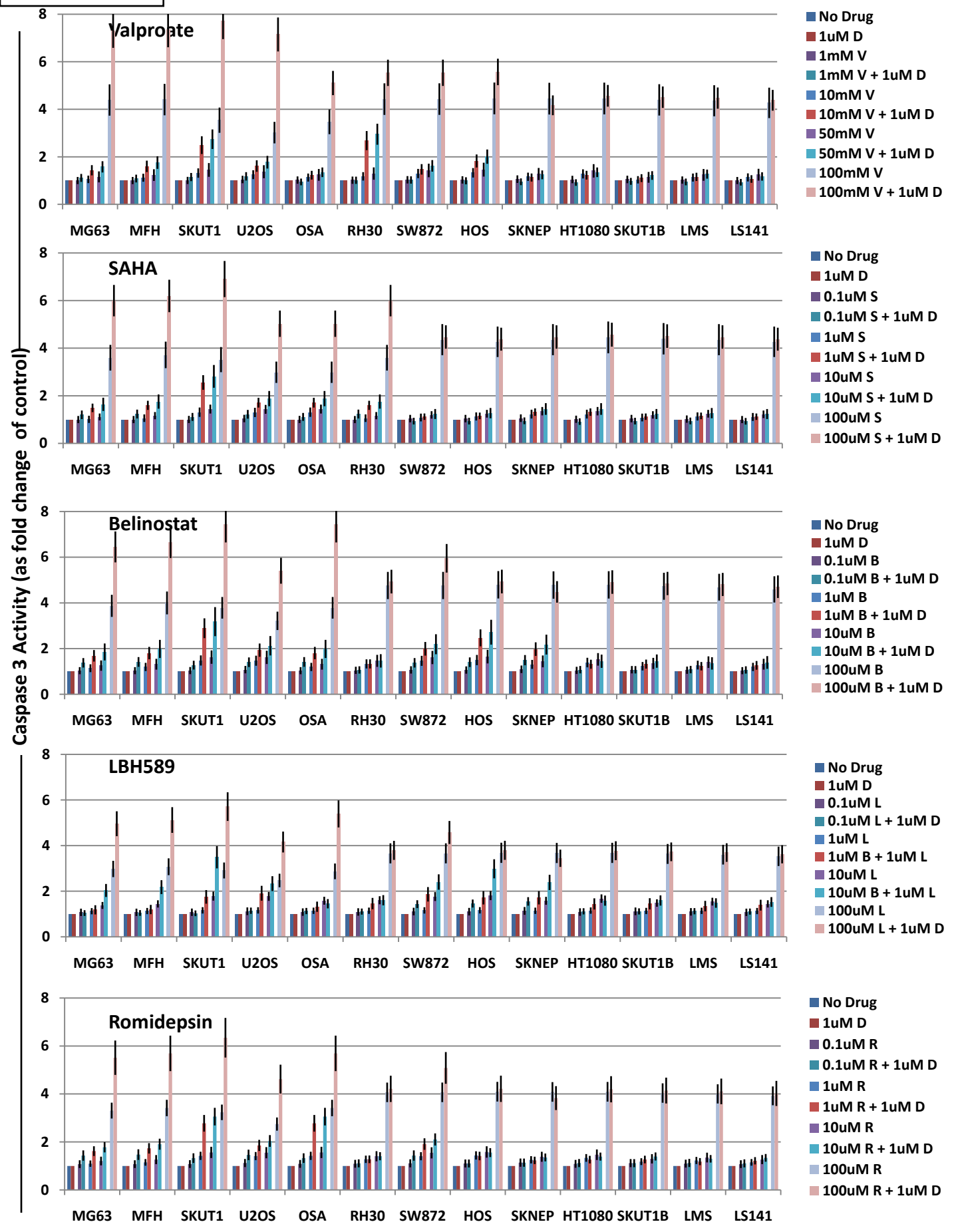

Supplemental FIGURE 6:

H&E

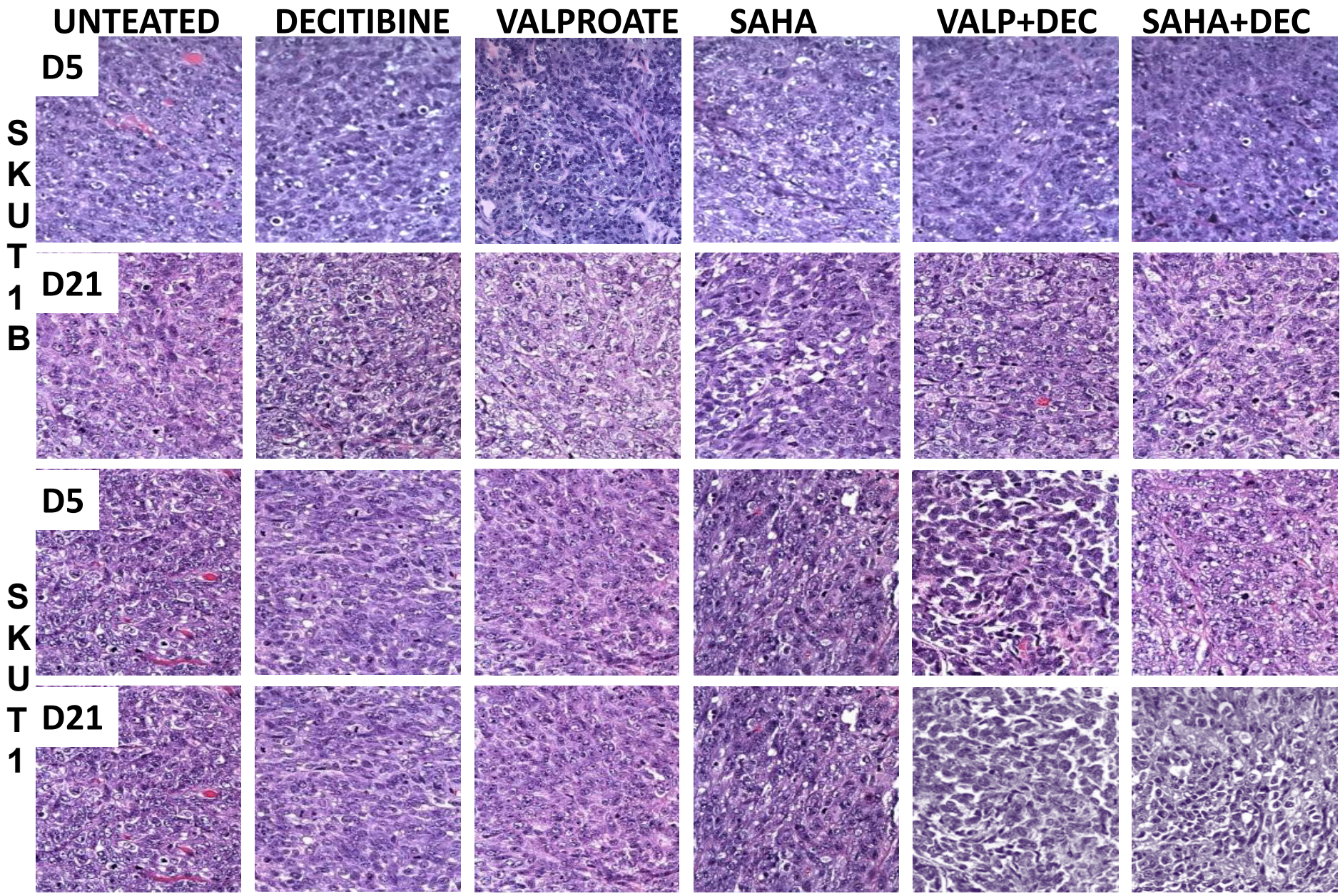

Supplemental FIGURE 7:

Ki67

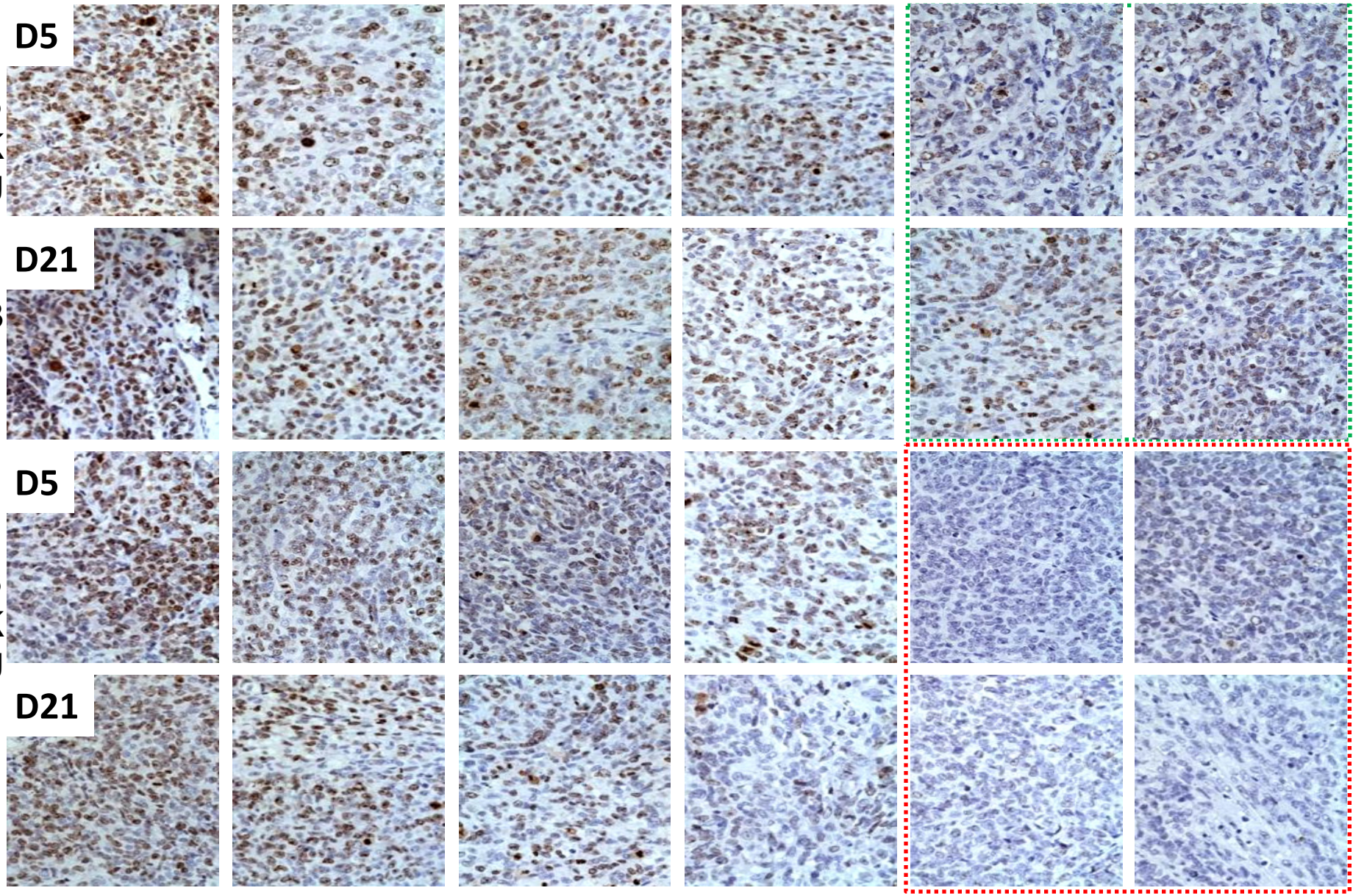

Supplemental FIGURE 8:

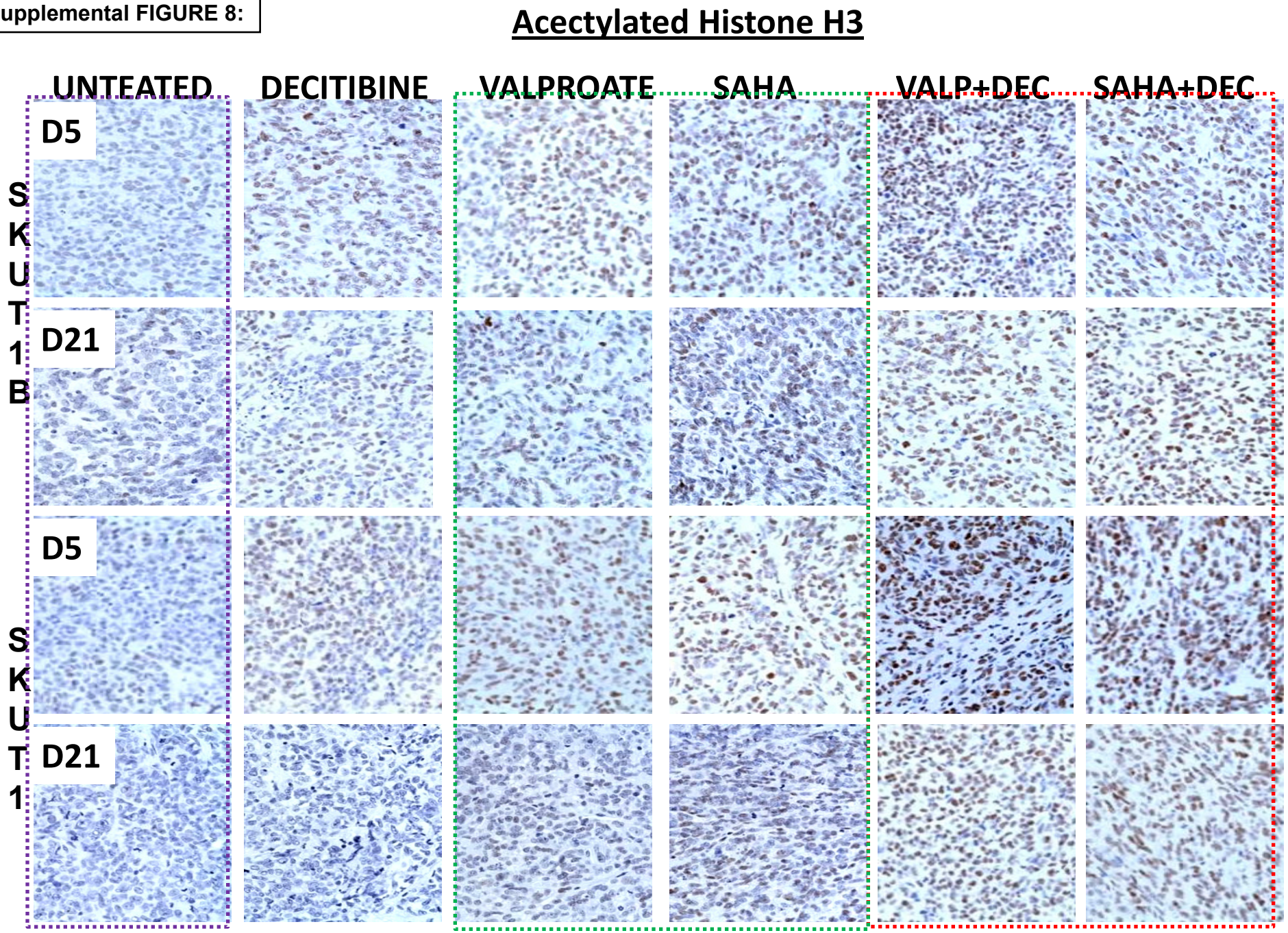

Supplemental FIGURE 9:

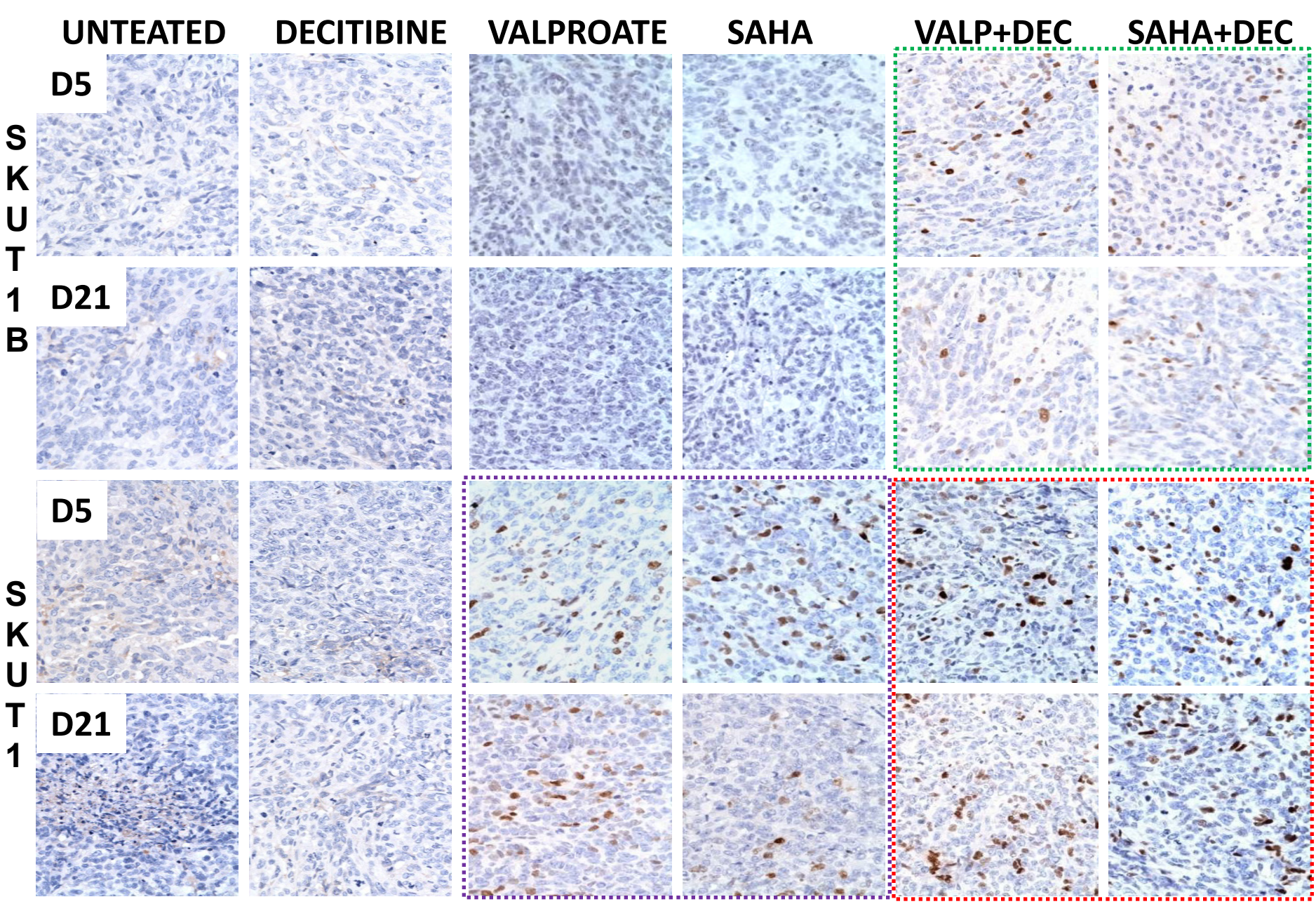

SUPPLEMENTAL FIGURE 10:

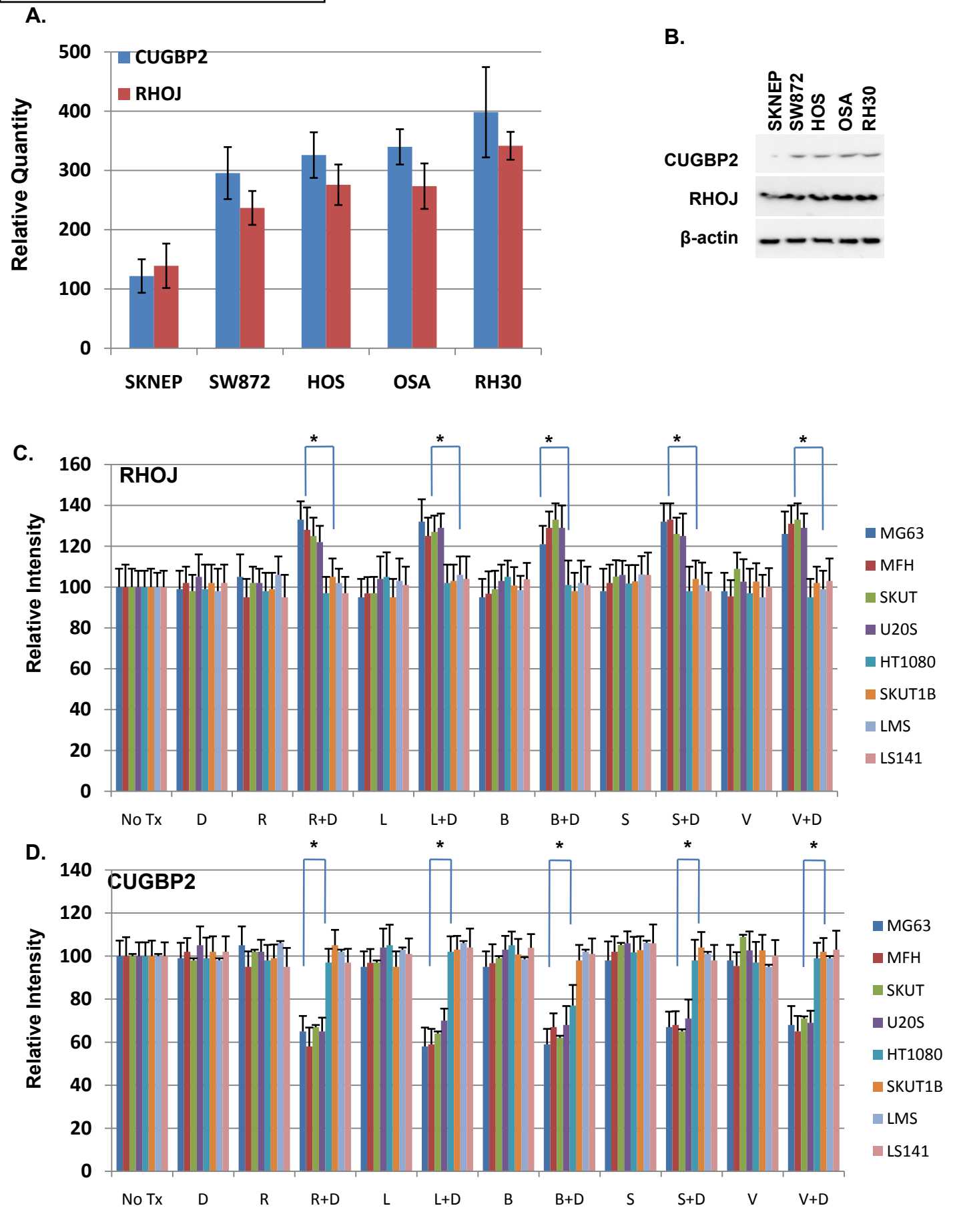

SUPPLEMENTAL FIGURE 11:

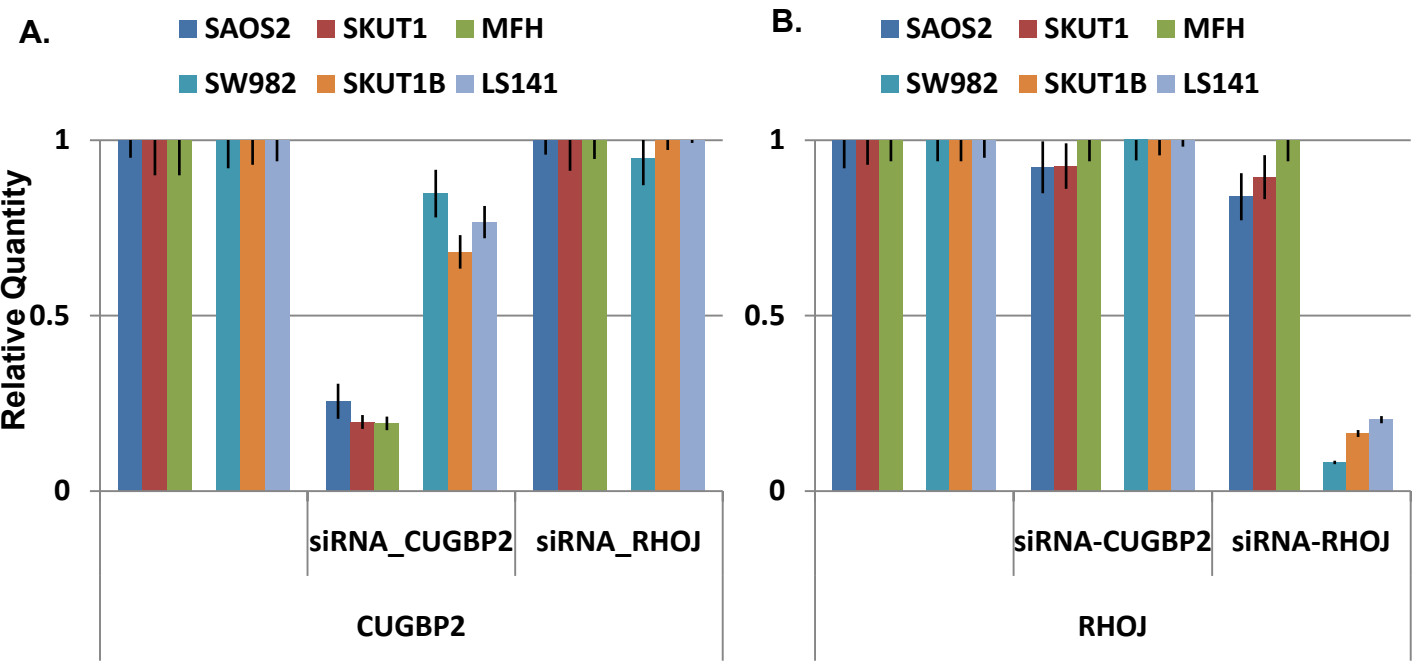

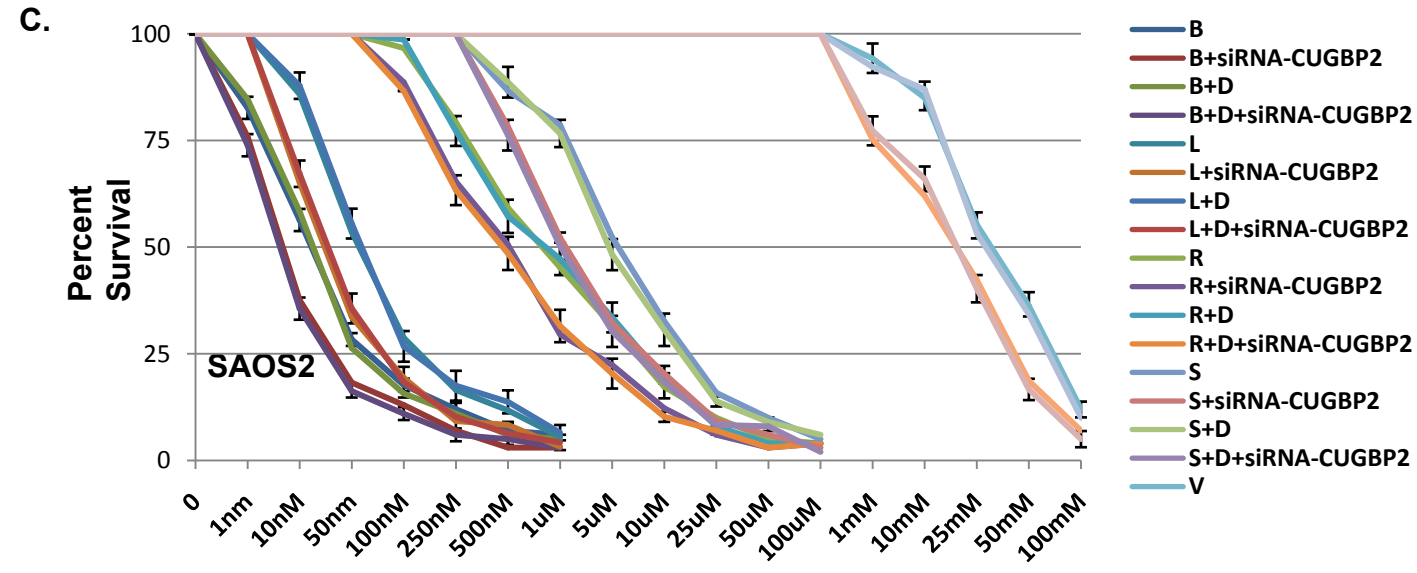

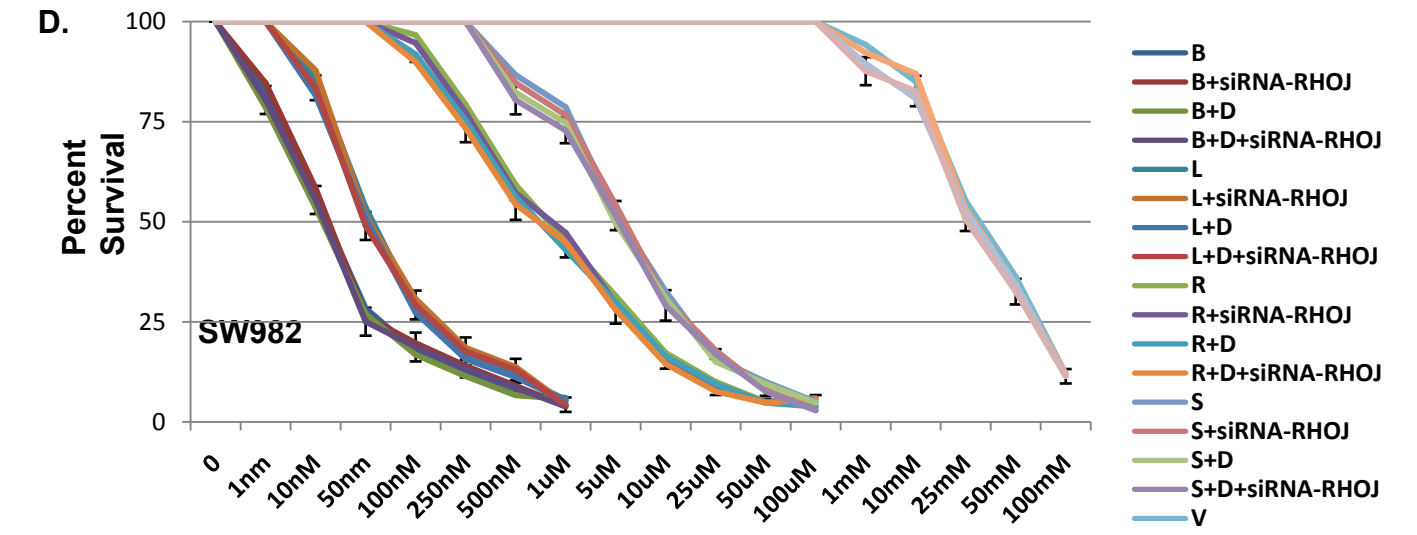

Mills et al.
Supplemental Table 1:

HDACI Published Sensitivity:

SAHA (Vorinostat) (1-4)

Pancreatic	0.8-5uM (IC50)
HBC-5 (breast cancer)	17 μM (GI50)
SNB-78 (CNS)	16 μM
HCT116 (colon cancer)	0.58 μM
DMS114 (lung cancer)	2.9 μM
LOX-IMVI (melanoma)	1.3 μM
SK-OV-3 (ovarian cancer)	2.5 μM
RXF-631 L (renal cancer)	2.0 μM
MKN45 (stomach cancer)	7.3 μM
PC-3 (prostate cancer)	4.6 μM
Sarcoma (MES-SA, SW1353, RCS, OUMS-27, SKES, WE68, RD, RH30)	0-10uM

Valproate (5-9)

BT4Cn -Rat Glioma	2.37-2.98 mM
N2a -Mouse neuroblastoma	2.11-3.19 mM
CSML0 -Mouse adenocarcinoma	0.94-1.08 mM
CAML100 -Mouse adenocarcinoma	0.98-1.41 mM
HeLa -Human adenocarcinoma	2.54-3.01 mM
L929 -Mouse fibroblastoid	0.97-1.29 mM
Breast (MCF-7 and MDA-231)	5.00-100 mM
Sarcoma (MG63, U20S, HOS, SAOS2, ESS-1, HT1080)	5.00-50.0 mM

Romidepsin (Depsipeptide) (10-12)

Cutaneous T-cell lymphoma (CTCL)	2-4 nM
Sarcoma (HOS,U2OS, HS-SY-2, SYO-I, SAOS2, YaFuSS)	10-20nM

Belinostat (PXD101) (13, 14)

Ovarian cancer	0.96 uM
Colorectal cancer	0.28 uM

LBH589 (Panobinostat) (15, 16)

breast cancer	<25nM
prostate cancer	10nM

REFERENCES:

1. He R, Chen Y, Ougolkov AV, Zhang JS, Savoy DN, Billadeau DD, et al. Synthesis and biological evaluation of triazol-4-ylphenyl-bearing histone deacetylase inhibitors as anticancer agents. J Med Chem. 2010;53:1347-56.
2. Hrzenjak A, Moinfar F, Kremser ML, Strohmeier B, Petru E, Zatloukal K, et al. Histone deacetylase inhibitor vorinostat suppresses the growth of uterine sarcomas in vitro and in vivo. Mol Cancer. 2010;9:49.
3. Yamamoto S, Tanaka K, Sakimura R, Okada T, Nakamura T, Li Y, et al. Suberoylanilide hydroxamic acid (SAHA) induces apoptosis or autophagy-associated cell death in chondrosarcoma cell lines. Anticancer Res. 2008;28:1585-91.

Mills et al.
Supplemental Table 1:

4. Sonnemann J, Dreyer L, Hartwig M, Palani CD, Hong le TT, Klier U, et al. Histone deacetylase inhibitors induce cell death and enhance the apoptosis-inducing activity of TRAIL in Ewing's sarcoma cells. J Cancer Res Clin Oncol. 2007;133:847-58.
5. Gotfryd K, Skladchikova G, Lepekhin EA, Berezin V, Bock E, Walmod PS. Cell type-specific anti-cancer properties of valproic acid: independent effects on HDAC activity and Erk1/2 phosphorylation. BMC Cancer. 2010;10:383.
6. Jawaid K, Crane SR, Nowers JL, Lacey M, Whitehead SA. Long-term genistein treatment of MCF-7 cells decreases acetylated histone 3 expression and alters growth responses to mitogens and histone deacetylase inhibitors. J Steroid Biochem Mol Biol. 2010;120:164-71.
7. Yamanegi K, Yamane J, Hata M, Ohyama H, Yamada N, Kato-Kogoe N, et al. Sodium valproate, a histone deacetylase inhibitor, decreases the secretion of soluble Fas by human osteosarcoma cells and increases their sensitivity to Fas-mediated cell death. J Cancer Res Clin Oncol. 2009;135:879-89.
8. Hrzenjak A, Moinfar F, Kremser ML, Strohmeier B, Staber PB, Zatloukal K, et al. Valproate inhibition of histone deacetylase 2 affects differentiation and decreases proliferation of endometrial stromal sarcoma cells. Mol Cancer Ther. 2006;5:2203-10.
9. Chavez-Blanco A, Perez-Plasencia C, Perez-Cardenas E, Carrasco-Legleu C, Rangel-Lopez E, Segura-Pacheco B, et al. Antineoplastic effects of the DNA methylation inhibitor hydralazine and the histone deacetylase inhibitor valproic acid in cancer cell lines. Cancer Cell Int. 2006;6:2.
10. Newbold A, Lindemann RK, Cluse LA, Whitecross KF, Dear AE, Johnstone RW. Characterisation of the novel apoptotic and therapeutic activities of the histone deacetylase inhibitor romidepsin. Mol Cancer Ther. 2008;7:1066-79.
11. Matsubara H, Watanabe M, Imai T, Yui Y, Mizushima Y, Hiraumi Y, et al. Involvement of extracellular signal-regulated kinase activation in human osteosarcoma cell resistance to the histone deacetylase inhibitor FK228 [(1S,4S,7Z,10S,16E,21R)-7-ethylidene-4,21-bis(propan-2-yl)-2-oxa-12,13-dithia-5,8,20,23-tetraazabicyclo[8.7.6]tricos-16-ene-3,6,9,19,22-pentone]. J Pharmacol Exp Ther. 2009;328:839-48.
12. Ito T, Ouchida M, Morimoto Y, Yoshida A, Jitsumori Y, Ozaki T, et al. Significant growth suppression of synovial sarcomas by the histone deacetylase inhibitor FK228 in vitro and in vivo. Cancer Lett. 2005;224:311-9.
13. Qian X, LaRochelle WJ, Ara G, Wu F, Petersen KD, Thougaard A, et al. Activity of PXD101, a histone deacetylase inhibitor, in preclinical ovarian cancer studies. Mol Cancer Ther. 2006;5:2086-95.
14. Tumber A, Collins LS, Petersen KD, Thougaard A, Christiansen SJ, Dejligbjerg M, et al. The histone deacetylase inhibitor PXD101 synergises with 5-fluorouracil to inhibit colon cancer cell growth in vitro and in vivo. Cancer Chemother Pharmacol. 2007;60:275-83.
15. Chen S, Ye J, Kijima I, Evans D. The HDAC inhibitor LBH589 (panobinostat) is an inhibitory modulator of aromatase gene expression. Proc Natl Acad Sci U S A. 2010;107:11032-7.
16. Verheul HM, Salumbides B, Van Erp K, Hammers H, Qian DZ, Sanni T, et al. Combination strategy targeting the hypoxia inducible factor-1 alpha with mammalian target of rapamycin and histone deacetylase inhibitors. Clin Cancer Res. 2008;14:3589-97.

Supplemental Table 2:

	Array id	Class label (Synergy)	Compound Covariate Predictor Correct?	Diagonal Linear Discriminant Analysis Correct?	1-Nearest Neighbor Correct?	3-Nearest Neighbors Correct?	Nearest Centroid Correct?	Support Vector Machines Correct?	Bayesian Compound Covariate Predictor Correct?
1	HT1080	N	2	YES	YES	YES	YES	YES	YES
2	LS141	N	2	YES	YES	YES	YES	YES	YES
3	SKLMS1	N	2	YES	YES	YES	NO	YES	YES
4	SKUT1B	N	2	YES	YES	YES	YES	YES	YES
5	MFH	Y	2	YES	NO	YES	YES	YES	YES
6	MG63	Y	2	YES	YES	YES	YES	YES	YES
7	SKUT1	Y	2	YES	YES	YES	YES	YES	YES
8	U2OS	Y	2	YES	YES	YES	YES	YES	YES
Mean percent of correct classification				100	88	100	88	100	100

Description of the problem:

Number of classes: 2
Number of genes used for random variance estimation: 28002
Number of genes that passed filtering criteria: 2
Column of the Experiment Descriptors sheet that defines class variable: synergy
Number of arrays in each class: 4 in class label *n* , 4 in class label *y*
Random Variance Model was used

Feature selection criteria:

Genes significantly different between the classes at the 0.01, 0.005, 0.001 and 0.0005 significance levels were used to build four predictors. The predictor with the lowest cross-validation mis-classification rate was selected. The best compound covariate classifier consisted of genes significantly different between the classes at the 0.001 significance level. The best diagonal linear discriminant analysis classifier consisted of genes significantly different between the classes at the 0.001 significance level. The best 1-nearest neighbor classifier consisted of genes significantly different between the classes at the 0.005 significance level. The best 3-nearest neighbors classifier consisted of genes significantly different between the classes at the 0.001 significance level. The best nearest centroid classifier consisted of genes significantly different between the classes at the 0.001 significance level. The best support vector machines classifier consisted of genes significantly different between the classes at the 0.005 significance level. The best Bayesian compound covariate classifier consisted of genes significantly different between the classes at the 0.001 significance level.
Only genes with the fold-difference between the two classes exceeding 2 were used for class prediction.